JOURNAL OF AIRCRAFT
Vol. 47, No. 1, January–February 2010

Fatigue-Based Severity Factors for Shear-Loaded Fastener Joints

S. Keshavanarayana,* B. L. Smith,† C. Gomez,‡ and F. Caido§
Wichita State University, Wichita, Kansas 67260-0044
M. Shiao¶
Federal Aviation Administration, Atlantic City International Airport, New Jersey 08405
and
M. Nuss**
Federal Aviation Administration, Kansas City, Missouri 64106

DOI: 10.2514/1.44588

Using Hi-Lok fasteners and Universal rivets, we experimentally investigated the fatigue behavior of fastener joints under constant-amplitude loading. The study generated fatigue-based stress severity factors for fastener joints at two different load transfer and mean stress levels. Fatigue tests on open-hole, filled-hole, and load transfer specimens were conducted at mean stress levels of 20.68 and 41.37 MPa, with varying stress ratios to achieve lives ranging between 10^3 and 10^6 cycles. The regression-based mean life curves were used to generate the fatigue-based correction factors for hole filling and bearing load transfer as a function of the maximum stress level. The fatigue life of load transfer specimens fell between those of the open-hole and filled-hole configurations. With increasing load transfer and mean stress levels, the fatigue life approached that of the open-hole case. In addition, at stress levels corresponding to fatigue lives in excess of 10^5 cycles, the failure modes of load transfer specimens transitioned from a net-section failure to a clamp-up-induced fretting failure occurring away from the fastener hole. The stress severity factor associated with the mean life of fastener joints and Hi-Lok filled-hole coupons increased with the maximum fatigue stress level. However, different trends were observed with respect to load transfer at the two mean stress levels used in the study.

Nomenclature

A, B	=	constants
d	=	diameter, mm
K_{tb}	=	bearing stress concentration factor
K_{tg}	=	stress concentration factor based on gross stress
n	=	fatigue life, cycles
P, ΔP	=	force, N
R	=	stress ratio
$S_{\max}$	=	maximum gross area stress, MPa
S_{mean}	=	mean gross area stress, MPa
t	=	sheet thickness, mm
w	=	width, mm
α, β, θ	=	empirical factors
ε	=	strain
σ	=	stress, MPa

I. Introduction

THE fatigue behavior of fastener joints has received widespread attention for several years due to its extensive use in metallic airframe structures. The fastener joints serve the primary purpose of transferring loads across structural members through bearing and by clamp-up-induced friction. Most fatigue-related failures initiate from fastener holes from the presence of higher stress levels associated with stress concentrations due to bypass loading and the load transfer. To improve joint performance, various investigations [1–7] have addressed issues such as hole quality, fastener type, interference, cold working, etc. A worldwide experimental exercise [7] on fatigue behavior of different types of fasteners and joints under spectrum loading concluded that load transfer level and secondary bending are key factors affecting a joint's fatigue life.

The lives of fastener joints under constant-amplitude fatigue have been shown to depend on the amount of load transfer. Lee [8] investigated the behavior of 7075-T7351 aluminum fastened by a traditional (nut–bolt) fastener under constant-amplitude fatigue loading ($R = 0.05$). The author observed a decrease in both crack initiation life and total fatigue life with increasing levels of load transfer. The degradation was conspicuous for the 100% load transfer case. At lower load transfer levels, the observed reduction in life was not distinct, due to the lack of sufficient data at each stress level. The results of spectrum tests on load transfer coupons reported in [7], however, do not exhibit a specific dependence of fatigue life on load transfer level, and the trends are affected by fastener types, sealants used at the faying surfaces, interference level, spectrum stress level, specimen design, and the different material systems of the parts being joined.

The clamp-up loads generated by the fasteners have a significant effect on the load transfer mechanisms, the resulting failure modes, and life under fatigue loading. Starikov [9] reported the influence of frictional forces arising due to fastener clamp-up on load transfer and fatigue life of fastener joints under spectrum loading. Using an instrumented fastener, the author measured the load transferred by bearing and due to friction at the faying surfaces. Although the total load transfer was observed to be more or less constant, the frictional load transfer was observed to increase with the number of spectrum loading blocks. The estimated coefficient of friction at the faying surfaces was observed to increase from about 0.2 to around 0.8 over 100 blocks of loading. The author observed fretting fatigue as the major mechanism inducing the initiation of fatigue fracture in the joint away from the fastener hole. According to Schijve [10], the high clamping generated by the fastener restrains the fretting around the hole, but secondary bending induces separation at the edge of the clamp region, leading to the fretting failure away from the hole.

Received 26 March 2009; revision received 22 July 2009; accepted for publication 21 August 2009.

*Assistant Professor, Department of Aerospace Engineering. Professional Member AIAA.
†Professor, Department of Aerospace Engineering. Professional Member AIAA.
‡Research Engineer, National Institute for Aviation Research.
§Research Assistant, Department of Aerospace Engineering.
¶Structural Integrity of Commuter Aircraft, William J. Hughes Technical Center.
**Continued Operational Safety Program Manager, Small Airplane Directorate.

Similar observations were reported by Wang [11], who used finite element models to indicate that the fretting crack initiation locations were along the stick-slip boundary. The stick-slip boundary for fasteners with high clamp-up loads was located away from the hole, whereas it intersected the hole boundary for riveted specimens, which have lower or negligible clamp-up loads.

The prediction methods for fatigue lives of fastener joints are typically conservative in nature due to the difficulty in modeling friction (specifically, its variation as a function of fatigue cycles [9] and the resulting effect on load transfer) and the interdependence of the various variables affecting the behavior of the joints [1]. The methods include the use of an effective stress concentration factor along with a damage-summation rule and crack-growth analysis. The use of effective stress concentration factors rely on the principle of similarity and superposition of the stresses due to bypass and bearing loads [12,13], whereas the crack-growth approaches assume crack nucleation at the fastener hole or the presence of an effective initial flaw for which the size is arrived at empirically [1,11]. Wang [11] explored the use of finite element model, which included contact, friction, and nonlinear material behavior to determine the stresses around fasteners in a mechanical joint. The author indicated that the presence of a shakedown condition contributes to a less severe fatigue state than predicted by the simple superposition of stresses [12,13]. Although the finite-element-based prediction tools are expedient for refining the fastener joint designs, a simpler fatigue-based tool would be desirable during the preliminary design stage.

The use of a *stress severity factor* (SSF) to characterize the fatigue quality of fastener joints has been reported by Jarfall [14]. The fatigue quality of fastener joint is expressed in terms of the SSF, which is given by [14]

$$\mathrm{SSF} = \frac{\alpha\beta}{\sigma_{\mathrm{ref}}}\left[K_{tb}\frac{\Delta P}{dt}\theta + K_{tg}\frac{P}{wt}\right] \tag{1}$$

where P is the bypass load and ΔP is the load transferred by the fastener/joint. The reference stress σ_{ref} could represent the remote (gross) stress in the part(s) being joined. The above equation is conceptually similar to those of [12,13] but also accounts for the fastener type, installation method, hole-preparation technique, and interference/clearance fit. The factor α is the hole-preparation factor that accounts for hole surface roughness and residual stresses from cold working, β is the hole-filling factor that accounts for the interference/clearance between the fastener and the hole, and θ is the bearing distribution factor that accounts for the effect of nonuniformity of bearing stress on the hole surface [14] due to bearing load eccentricity. In a complex joint involving multiple fasteners, the SSF can be used qualitatively to identify the most severely loaded fastener. A high SSF indicates that the particular fastener in the joint is vulnerable to fatigue failure.

For the factors α and β, reference conditions may be chosen arbitrarily. For instance, $\alpha = 1$ for a drilled hole of standard quality and $\beta = 1$ for an open hole [14]. The value of θ based on elastic analysis may be found in [15]. The stress severity factor based on elastic superposition provides a qualitative measure of the fatigue strength (or life) relative to that of an open-hole specimen. According to Jarfall [14], for the SSF to be used as fatigue factor, the empirical factors α, β, and θ must be developed from fatigue test data and will thus be dependent on the stress levels and the number of stress cycles. Fatigue tests on open-hole, filled-hole, and load transfer specimens are required to develop these empirical factors [14]. The fatigue-based factors will account for the differences in the damage accumulated due to factors such as clamping, friction, etc., which is not captured by the bearing and bypass stress concentration terms. The SSF obtained using the fatigue-based empirical factors represents the fatigue strength reduction factor or the fatigue factor relative to the open-hole configuration. The SSF for an open-hole configuration (with a certain hole surface quality: say, drilled) is assigned a value equal to its K_{tg}.

Although the effects of load transfer on the fatigue life of specific fastener joints under constant amplitude [8] and spectrum loading [1,7,9] have been reported in literature, no attempts have been made to develop the aforementioned empirical factors based on the fatigue data. It is envisaged that the empirical factors (specifically, θ) will exhibit a relationship with the load transfer and fatigue stress levels [14]. In addition, the constant-amplitude fatigue data reported in literature is mostly for positive stress ratios [8], in which the stress concentration due to bypass and bearing loads are cumulative [12,13]. In the current study, the constant-amplitude fatigue behavior of open-hole, filled-hole, and single-lap fastener joint specimens have been investigated experimentally. The objective of the present work was to generate experimentally based fatigue factors that capture the effects of hole quality, hole filling, and load transfer level. The fatigue factors in conjunction with a damage-summation rule could be used to obtain a quick estimate of the fatigue life of a fastener joint. The hole-preparation factor is established by conducting limited number of tests on open-hole specimens with different hole-preparation methods. The empirical factors β and θ have been developed using fatigue tests conducted on open-hole, filled-hole, and load transfer specimens. The nominal load transfer levels addressed in this study are 30% [intermediate load transfer (ILT)] and 50% [medium load transfer (MLT)]. The details of the experimental program, results, and observations are presented in this paper. The test data generated in this study could potentially be used for estimating the fatigue lives of fastener joints with comparable load transfer and stress levels using a damage-summation rule. In addition, the dependence of fretting failure (occurring away from the hole) on the fatigue stress level will be captured in this program. The experimental data could also be used for development/verification of computational models in the future.

II. Methodology

The fatigue-based factors α, β, and θ may be obtained by assuming that the fatigue strength for a given life is inversely proportional to the SSF [14]. The fatigue strength for a given life may be written as

$$S_{\mathrm{MAX}}(n) \propto \frac{1}{\mathrm{SSF}} \tag{2}$$

Since the severity factors are defined relative to the open-hole configuration [14], the ratio of fatigue strengths of the open-hole configuration (OH) and some other configuration ($*$) for which SSF is desired may be written as

$$\frac{S^{\mathrm{OH}}_{\mathrm{MAX}}(n)}{S^{*}_{\mathrm{MAX}}(n)} = \frac{\mathrm{SSF}^{*}}{\mathrm{SSF}^{\mathrm{OH}}} \tag{3}$$

The above equation requires that the fatigue strength be determined at specific lives. However, the fatigue life is the dependent variable in fatigue experiments, and thus the fatigue strength has to be expressed as a function of life. Using the test data for different specimen configurations, the fatigue-based empirical factors may be obtained systematically [14]. To obtain a measure of the effects of hole quality, open-hole specimens with different hole-preparation methods are subjected to fatigue testing at desired stress levels, and the fatigue data is used to express fatigue strength as a function of life using curve fitting. If the simple drilled hole is used as a baseline configuration ($\alpha = 1$), then the hole-preparation factor for other preparation methods may be determined using Eq. (3) as

$$\alpha^{*}(n) = \frac{S^{\mathrm{OH-DRL}}_{\mathrm{MAX}}(n)}{S^{*}_{\mathrm{MAX}}(n)}\alpha = \frac{S^{\mathrm{OH-DRL}}_{\mathrm{MAX}}(n)}{S^{*}_{\mathrm{MAX}}(n)} \tag{4}$$

In the above equation, $S^{\mathrm{OH-DRL}}_{\mathrm{MAX}}$ represents the fatigue strength of open-hole specimen with drilled hole.

To obtain the hole-filling factor β, for a particular fastener type and interference/clearance level, fatigue data for filled-hole specimens are generated. Using the open- and filled-hole fatigue data, Eq. (3) may be written as

$$\frac{S^{\mathrm{OH}}_{\mathrm{MAX}}(n)}{S^{\mathrm{FH}}_{\mathrm{MAX}}(n)} = \frac{\mathrm{SSF}^{\mathrm{FH}}}{\mathrm{SSF}^{\mathrm{OH}}} \tag{5}$$

where the superscript FH represents filled-hole configuration. The SSFs can be expressed in terms of the stress concentration factor K_{tg} and the factors α and β, as follows:

$$\frac{S^{\mathrm{OH}}_{\mathrm{MAX}}(n)}{S^{\mathrm{FH}}_{\mathrm{MAX}}(n)} = \frac{\alpha_{\mathrm{FH}}\beta_{\mathrm{FH}}(K_{tg})_{\mathrm{FH}}}{\alpha_{\mathrm{OH}}\beta_{\mathrm{OH}}(K_{tg})_{\mathrm{OH}}} \tag{6}$$

Since $\alpha_{\mathrm{OH}} = \beta_{\mathrm{OH}} = 1$ for the reference configuration and $\alpha_{\mathrm{FH}} = a^*(n)$, the above equation simplifies to

$$\beta_{\mathrm{FH}}(n) = \frac{1}{\alpha^*(n)} \times \frac{S^{\mathrm{OH}}_{\mathrm{MAX}}(n)}{S^{\mathrm{FH}}_{\mathrm{MAX}}(n)} \tag{7}$$

In the above equation, the stress concentration factor is assumed to be the same for the OH and FH configurations. The determination of the bearing factor θ follows the same procedure used for the hole-filling factor. The ratio of the fatigue strengths of a load transfer and open-hole configurations can be written as

$$\frac{S^{\mathrm{OH}}_{\mathrm{MAX}}(n)}{S^{\mathrm{LT}}_{\mathrm{MAX}}(n)} = \frac{\alpha_{\mathrm{LT}}\beta_{\mathrm{LT}}}{\alpha_{\mathrm{OH}}\beta_{\mathrm{OH}}(K_{tg})_{\mathrm{OH}}}\left[K_{tb}\left(\frac{\Delta P}{P+\Delta P}\right)\frac{w}{d}\theta + (K_{tg})_{\mathrm{LT}}\left(\frac{P}{P+\Delta P}\right)\right] \tag{8}$$

where

$$\alpha_{\mathrm{LT}} = \alpha_{\mathrm{FH}} = \alpha^*(n) \qquad \beta_{\mathrm{LT}} = \beta_{\mathrm{FH}}(n) \qquad (K_{tg})_{\mathrm{LT}} \approx (K_{tg})_{\mathrm{OH}}$$

and

$$\frac{\Delta P}{P+\Delta P} = \mathrm{LT}$$

is the nominal load transfer level.

Equation (8) along with Eq. (7) may be combined to obtain an expression for θ, which is given by the following equation:

$$\theta(n) = \left(\frac{K_{tg}}{K_{tb}}\right)\left(\frac{d}{w}\right)\left(\frac{1}{\mathrm{LT}}\right)\left[\frac{S^{\mathrm{FH}}_{\mathrm{MAX}}(n)}{S^{\mathrm{LT}}_{\mathrm{MAX}}(n)} - (1-\mathrm{LT})\right] \tag{9}$$

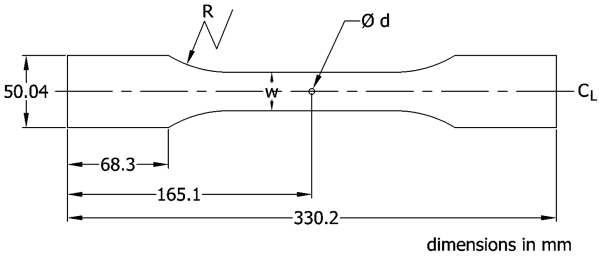

Fig. 1 Specimen geometry for open- and filled-hole tests.

Using the above equation and the nominal load transfer level, the factor θ may be expressed as a function of life or maximum stress under fatigue loading. The fatigue-based empirical factors obtained using the equations presented in this section will be dependent on the choice of mean stress, stress ratio, fastener type, and specimen material.

III. Experiments

A. Materials and Specimen Geometry

Three specimen types (open-hole, filled-hole, and load transfer specimens) were tested in this program to develop the empirical factors for the material. The test specimens were machined from 2024-T3 clad aluminum with a nominal thickness of 2.286 mm. The material has a nominal Young's modulus $E = 72.4$ GPa, Poisson's ratio $\nu = 0.33$, ultimate tensile strength $\sigma_{\mathrm{ULT}} = 427$ MPa, tensile yield strength $\sigma_y = 324$ MPa, ultimate shear strength $\tau_{\mathrm{ULT}} =$ 262 MPa, and bearing yield strength of 482 MPa [16].

The basic test-specimen geometry used for the open-hole and filled-hole specimens is dog-bone-shaped, as illustrated in Fig. 1. Two specimen widths, 19.05 and 38.1 mm, were used in the study. To prevent any inadvertent scratching of the clad layer during machining and handling of the specimen, all raw sheets were covered with a layer of cellophane tape before the machining process. The cellophane tape was removed after the specimens were completely machined and ready for testing. The fastener holes were drilled using a carbide drill bit at a nominal rotational speed of 1500 rpm. A Hi-Lok protruding shear head fastener (HL18 pin and HL70 collar) and Universal head rivets with nominal diameters of 4.127 mm were used in the present study. Thus, the fastener-diameter-to-sheet-thickness ratio used was 1.82. The holes in the open-hole and rivet filled-hole specimens were drilled holes, whereas the holes in Hi-Lok filled-hole specimens were drilled and reamed. Further, the holes in the load transfer specimens using rivets were drilled holes, whereas those using Hi-Lok fasteners were drilled and reamed. A clearance fit ($\sim$0.06 mm over the diameter) was used for specimens employing Hi-Lok fasteners.

To study the effects of hole quality, open-hole specimens with holes machined using four methods have been used. The hole-preparation methods used were drilled holes; drilled and reamed holes; drilled and deburred holes; and drilled, reamed and deburred holes. Oversized (6.35-mm-diam) drill bits were used to deburr the hole edge in a controlled manner.

The load transfer specimen assembly consists of a main (or bypass) part, which is the primary member (full dog bone), and a load transfer (or secondary/half dog bone) part. The load transfer specimen used in the current study is the widely reported 1.5-dog-bone specimen configuration [1,7,8], as illustrated in Fig. 2. The geometry of the load transfer part is illustrated in Fig. 3. The two parts are connected to each other using the fastener (under study) in the gauge section and constraint pins in the gripping region. Ensuring

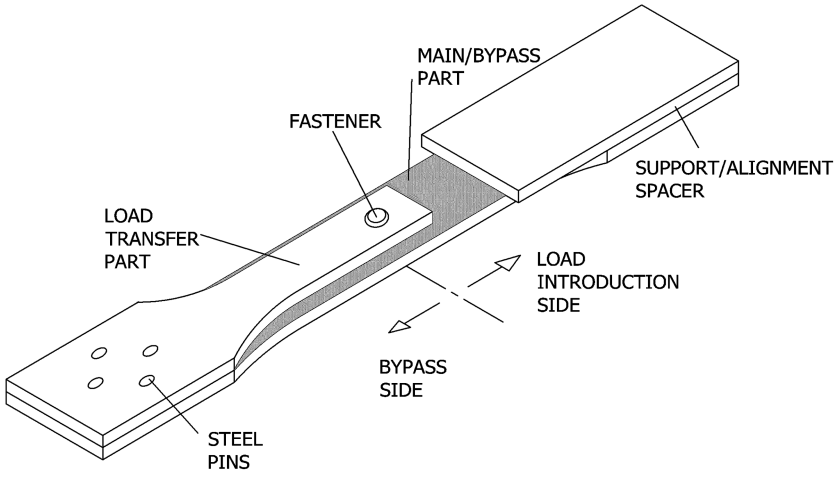

Fig. 2 Illustration of a load transfer specimen.

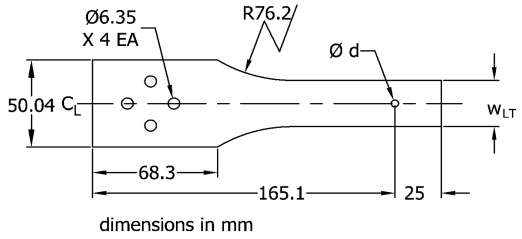

Fig. 3 Geometry of load transfer part.

compatibility of displacements in the grip region is necessary to enforce load transfer between the two parts [7]. The far-field loads are introduced into the main part of the assembly. Depending on the relative stiffness of the load transfer part, a specific amount of load is transferred to it via the fastener joint. The stiffness can be varied by altering the cross-sectional dimensions and the material itself. In the present study, the load transfer part and the main part were manufactured from the same material, and the stiffness of the load transfer parts were varied by using different widths. The widths of the main and load transfer parts of the ILT and MLT specimens are listed in Table 1. The displacement compatibility in the gripping region was achieved satisfactorily by using four 6.35-mm-diam steel pins, as illustrated in Fig. 2. This combination was arrived at by limited experimentation with different configurations.

B. Test Apparatus

The quasi-static and constant-amplitude fatigue tests were conducted using 24-kN-capacity MTS Systems Corporation (MTS) servo hydraulic load frames. The test control was accomplished using the Multipurpose TestWare computer program [17]. The test specimens were supported laterally along the gauge length to prevent global buckling under compression loading. The lateral supports consisted of aluminum plates between which the specimens were clamped, as shown in Fig. 4. The plates were fastened to the end of a beam cantilevered off the testing machine column, as shown in the same figure. To minimize the friction between the specimen and the supports, a layer of Teflon plastic was used between the specimens and the aluminum plates, as shown in the figure. Appropriate recesses were machined in the Teflon plastic layer to accommodate the fastener and strain gauges and to minimize the contact friction. To position the restraint supports, a dummy specimen with back-to-back strain gauges was used before mounting of the actual specimen. A small tensile load was applied to the specimen and the supports were positioned such that the bending of the specimen was negligible.

C. Load Transfer Characterization

The load transfer in the 1.5-dog-bone specimen occurs due to the enforced displacement compatibility between the main part and the load transfer part. If the fastener is assumed to be rigid and the bearing deformations are negligible, the amount of load transferred is purely a function of the relative longitudinal stiffnesses (over the length between the fastener and the gripped region) of the main part and the load transfer part. A simple mechanics-of-materials approach for determining the load transfer level for this idealized scenario has been reported by Park and Grandt [18]. However, owing to the deformation

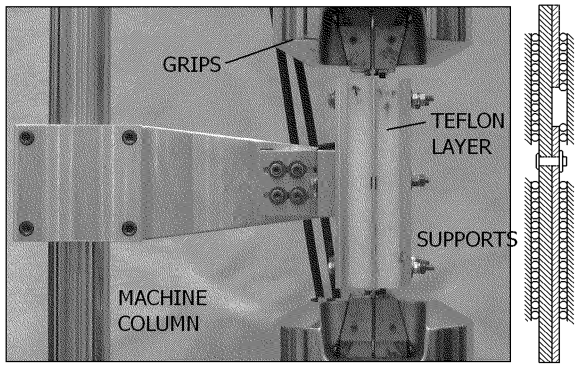

Fig. 4 Test fixture and schematic of the imposed constraints on the specimen.

of the hole, bending of fastener and rotation of the joint itself, the load transfer level will vary as a function of applied loading [1,7,19]. The presence of fastener clamp-up loads and hole clearance will further complicate the load transfer process, due to the participation of the frictional load transfer at the faying surfaces.

In the present study, the load transfer was characterized by conducting quasi-static tests on instrumented specimens. Since the far-field strains are elastic, they were used as a measure of load in the specimen. As the joint is unbalanced (single shear), secondary bending occurs and the strains are not uniform across the thickness of the two parts. Thus, back-to-back strain gauges (Vishay EA-06-250BG-120) were used, as shown in Fig. 5. A shallow groove (0.3 mm deep) was machined on the faying surface of the load transfer part to accommodate the strain gauge on the main part, as illustrated in Fig. 5.

The load transfer in the specimen was computed by using the following equation:

$$\%\ \text{load transfer} = \left[1 - \frac{\varepsilon_C + \varepsilon_D}{\varepsilon_A + \varepsilon_B}\right] \times 100 \tag{10}$$

The above equation provides the total load transferred by the joint. However, it cannot resolve the load transferred by the fastener and due to clamping-induced friction at the faying surfaces [1]. The secondary bending in load transfer specimens was characterized by using the secondary bending ratio [2,7], which is defined as

$$\text{secondary bending ratio} = \begin{cases} \frac{\varepsilon_A - \varepsilon_B}{\varepsilon_A + \varepsilon_B} \sim \text{load introduction side} \\ \frac{\varepsilon_C - \varepsilon_D}{\varepsilon_C + \varepsilon_D} \sim \text{bypass side} \end{cases} \tag{11}$$

The secondary bending ratios are reported on the two sides of the joint, due to the differences in constraints existing at the two locations. The secondary bending has been typically reported at specific points across the minimum section adjacent to the hole, often referred to as AGARD points [7]. However, owing to the small size of the fastener, it would be difficult to mount gauges at locations close to the fastener, and machining of shallow grooves at the corresponding locations on the load transfer part could significantly alter its local stiffness and thus affect the load transfer itself.

Table 1 Nominal dimensions of test specimens

Specimen type	Fastener type	Nominal hole diameter d, mm	Width of main part w, mm	Width of load transfer part w_{LT}, mm	Nominal load transfer level
OH	None	4.08	38.10[a]	——	——
FH	Hi-Lok	4.19	38.10	——	——
FH	Rivet	4.08	38.10	——	——
ILT	Hi-Lok	4.19	38.10	26.67	30%
MLT	Hi-Lok	4.19	38.10	38.1	50%
MLT	Rivet	4.08	19.05	19.05	50%

[a]A width of 19.05 mm was used to study the effects of hole-surface-preparation quality.

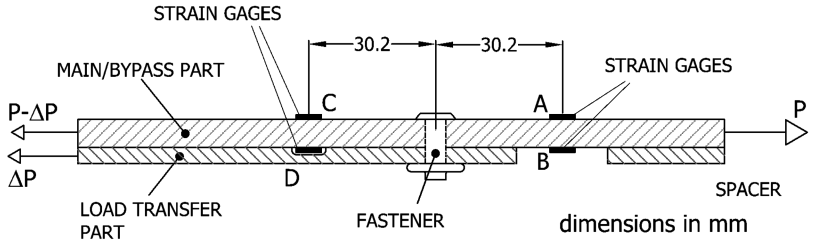

Fig. 5 Specimen instrumentation for load transfer measurement.

D. Fatigue Testing

The constant-amplitude fatigue tests were conducted using 24-kN-capacity MTS servo hydraulic load frames. A minimum of six specimens were tested at each maximum stress level to facilitate statistical analysis of the fatigue-life data. The number of cycles to failure and failure modes were recorded for each test. The test specimens were fatigued at mean stress levels of 20.68 and 41.37 MPa and at a frequency of 20 Hz. The test frequency was reduced to 10 Hz for the higher stress amplitudes. The maximum stress levels were varied to achieve fatigue failure in the ranges of 10^3–10^4, 10^4–10^5, 10^5–10^6, and 10^6–10^7 cycles.

IV. Results and Discussion

A. Load Transfer Characterization

The variation of load transfer in ILT and MLT specimens was characterized by subjecting the specimens to a single tension–compression cycle. Lateral restraint supports were used to prevent global buckling during the compression phase of the test and to keep the constraints similar to those of the fatigue tests. The variation of load transfer in the MLT test specimens subjected to a tension–compression loading cycle is shown in Figs. 6 and 7 for specimens with a Hi-Lok and rivets, respectively. The load transfer was observed to vary with the applied loading with a conspicuous initial drop in the load transferred, especially for the specimen using a Hi-Lok fastener. This can be attributed to the clearance hole used in the specimen. The friction at the faying surface dominates the initial load transfer process, and bearing load transfer takes over when the two parts slip relative to each other and the fastener engages the hole surface. The load transfer level stays slightly below 40% during the tensile loading phase, as shown in the figure. During the unloading phase, the load transfer level differs from that of the loading phase, due to the plastic deformation at the hole boundary and friction at the faying surface. Upon reloading in compression, a higher load transfer level (~50%) was observed. This is due to the stiffer constraint on the rotation of the fastener joint. Under compression loading, the hole diameter tends to reduce along the loading direction and thus grips the fastener, resulting in an increased constraint on the rotation of the joint. In addition, the increase in the thickness of the main and load transfer parts due to the Poisson effect results in a corresponding increase in the clamp-up force that further promotes frictional load transfer across the faying surfaces.

The load transfer levels attained for the MLT specimens with a rivets was slightly different in comparison to that of the Hi-Lok specimens. Under both tension and compression loading, a load transfer level of 40% was observed. The load transfer in Hi-Lok specimens would be expected to be higher than the riveted specimens, due to the higher joint stiffness emanating from stiffer fastener material and higher clamp-up loading. However, under tensile loading the load transfer levels are similar, probably due to the use of clearance fit for the Hi-Lok specimens and must be investigated further. Under compression loading, the aforementioned Poisson effects will be more dominant in the Hi-Lok specimens, due to the higher clamp-up loading, which results in a higher load transfer level in these specimens. It should also be noted that the actual magnitude of load transferred by the joint is different for specimens using Hi-Lok fasteners and rivets, due to the different w/d ratios used for these specimens. A smaller w/d ratio was used for the riveted specimens to avoid shearing of the rivets. The hysteresis behavior observed in the load transfer specimens must be further investigated to obtain a better understanding of the relative contributions of frictional load transfer and plastic deformation.

The influence of residual plastic deformation can significantly affect the load transfer under reversed loading. This is illustrated in Fig. 8 for an ILT specimen deliberately loaded to a gross stress level of 300 MPa in tension. At this load level, plastic deformation due to stress concentration as well as bearing yield occurs. The maximum load transfer level achieved under tensile loading is about 26%. However, the load transfer under subsequent compression loading does not reach the levels achieved under tensile loading. The enlarged hole due to plastic deformation, in addition to the originally existing clearance, results in poor load transfer response during the compression phase of the test. Additional tests at lower tensile and compression stress levels resulted in load transfer behavior similar to that of the MLT specimen (but with lower load transfer level: ~26%). Based on a limited number of fatigue tests (up to 1000 cycles) during which the strains were recorded, it was observed that the load transfer behavior stabilized after roughly 10 cycles. No significant change in

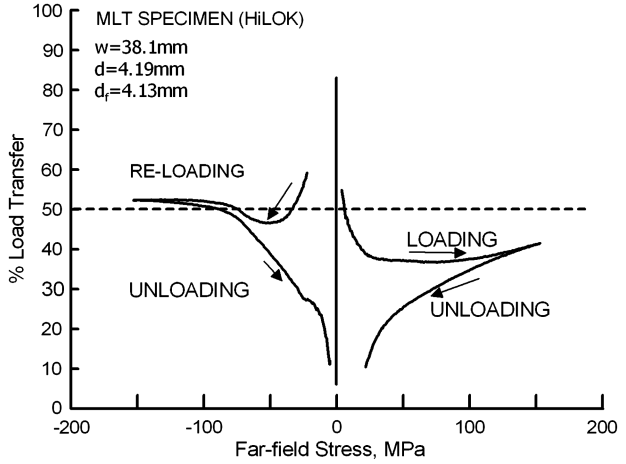

Fig. 6 Measured load transfer in a MLT specimen with a Hi-Lok fastener.

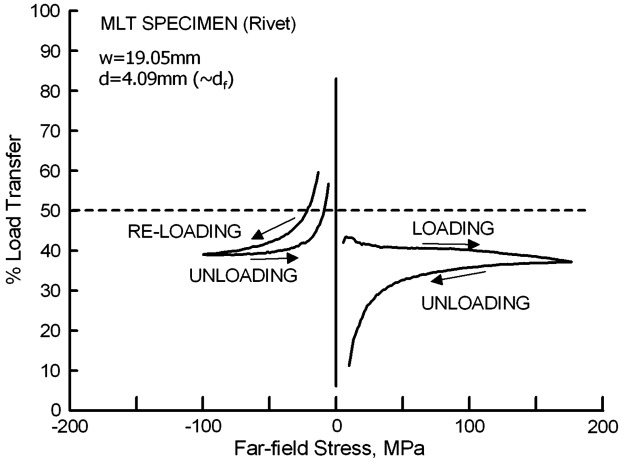

Fig. 7 Measured load transfer in a MLT specimen with a rivet.

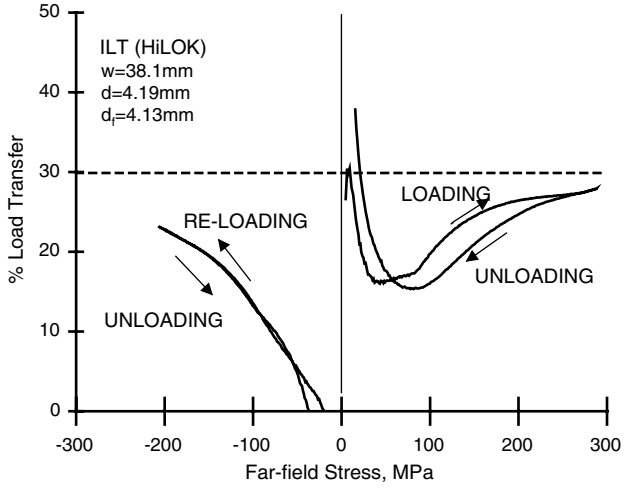

Fig. 8 Measured load transfer in a ILT specimen with a Hi-Lok fastener.

load transfer levels was observed during the subsequent loading cycles.

The secondary bending in MLT specimens based on strain gauge readings are plotted as a function of far-field stress in Figs. 9 and 10. The secondary bending levels observed in the specimens are consistent with the values reported in [7] for the 1.5-dog-bone specimen configuration. The lower secondary bending observed in riveted specimens is due to the narrower specimen, which results in a smaller load transferred by the rivets, even though the percentage transferred load remains the same. The variations of secondary bending observed in ILT specimens were similar to those observed in the riveted MLT specimen.

B. Fatigue Testing

The fatigue test data generated in this program were used for S–n characterization of the individual configurations and to generate the stress severity factors and associated fatigue-based empirical factors for the filled-hole and load transfer specimens. To obtain the fatigue-based empirical factors using the methodology described earlier, the fatigue test data for the open-hole, filled-hole, and load transfer specimens were characterized using a best-fit curve of the form

$$\log n = A + BS_{\mathrm{MAX}} \tag{12}$$

The above equation was fit to the experimental data by regressing over the log life [8]. The suspended test data and the data at

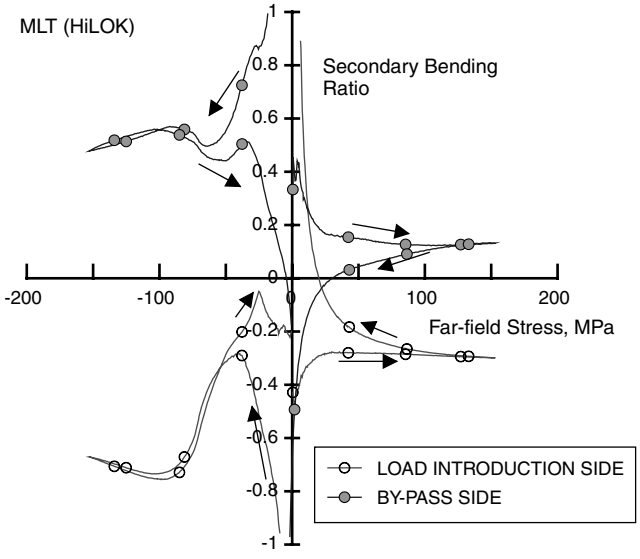

Fig. 9 Secondary bending in MLT specimen with a Hi-Lok fastener.

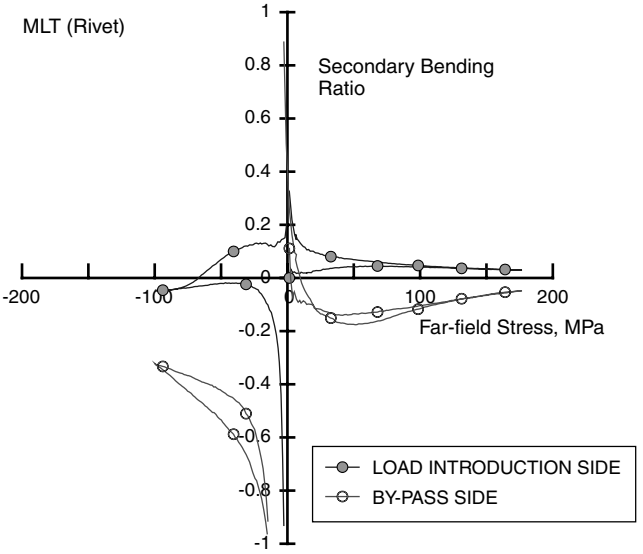

Fig. 10 Secondary bending in MLT specimen with a rivet.

exploratory stress levels were not included in the curve-fit process. The least-squares curve fit was carried out using the Table Curve 2D computer program [20]. It may be noted that similar stress-life curves could be generated for characteristic fatigue lives (e.g., B90, etc.) by using the maximum likelihood method, which captures the variation in fatigue life and its scatter as a function of the stress level [21,22]. The fatigue test data for the different specimen configurations along with the best-fit curves are plotted in Figs. 11–16.

To obtain a measure of the effects of hole quality, the limited fatigue test data on open-hole specimens for which the holes were drilled using four hole-preparation methods has been used. The hole-preparation methods used were drilled holes; drilled and reamed holes; drilled and deburred holes; and drilled, reamed and deburred holes. Three test specimens were tested for each combination of the hole-preparation method and the three maximum stress levels. A mean stress level of 41.36 MPa was used for these tests. The test data are summarized in Fig. 17. It may be observed that for the hole-preparation methods used in this study, no significant differences or trends exist. This implies that we could arbitrarily set $\alpha = 1$ for the different hole-preparation methods used in this study.

The fatigue lives of open-hole and filled-hole specimens with Hi-Lok fasteners and universal head rivets at mean stress levels of 20.68 and 41.36 MPa and at different S_{MAX} levels are presented along with

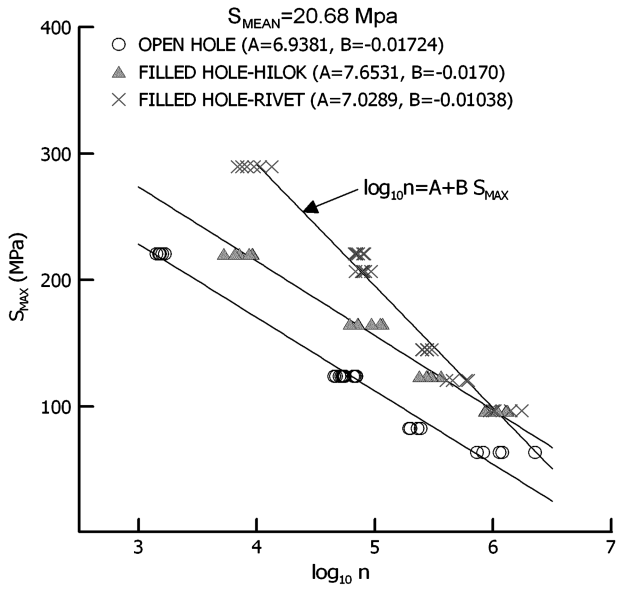

Fig. 11 Fatigue data and best-fit curves for open-hole and filled-hole configurations at $S_{\mathrm{mean}} = 20.68$ MPa.

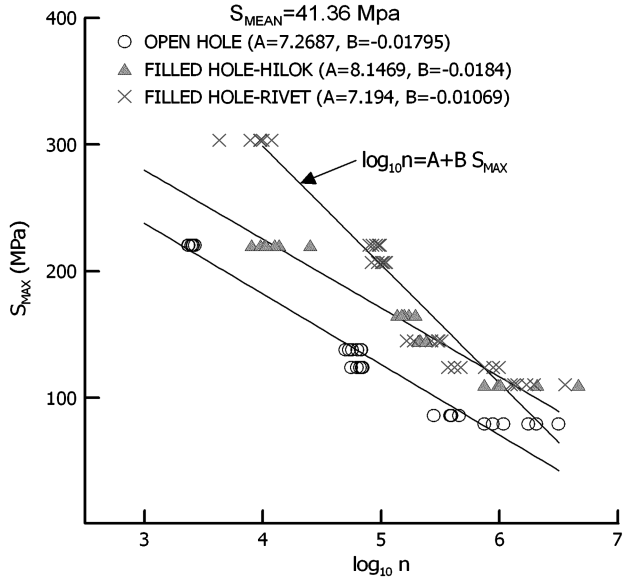

Fig. 12 Fatigue data and best-fit curves for open-hole and filled-hole configurations at $S_{mean} = 41.36$ MPa.

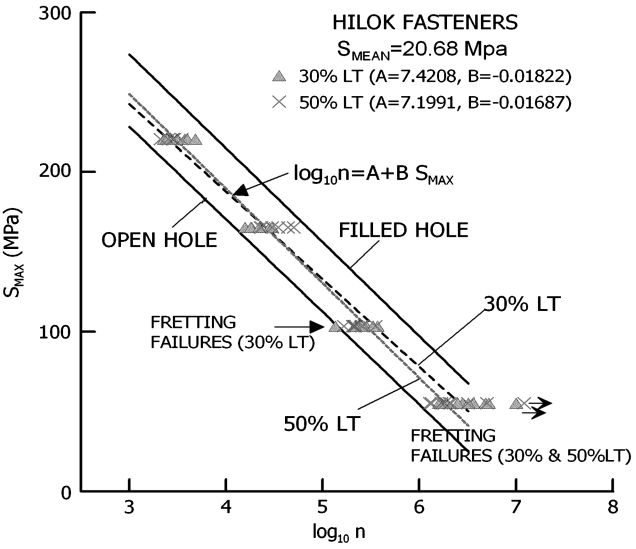

Fig. 13 Fatigue data and best-fit curves for load transfer specimens (Hi-Lok) at $S_{mean} = 20.68$ MPa.

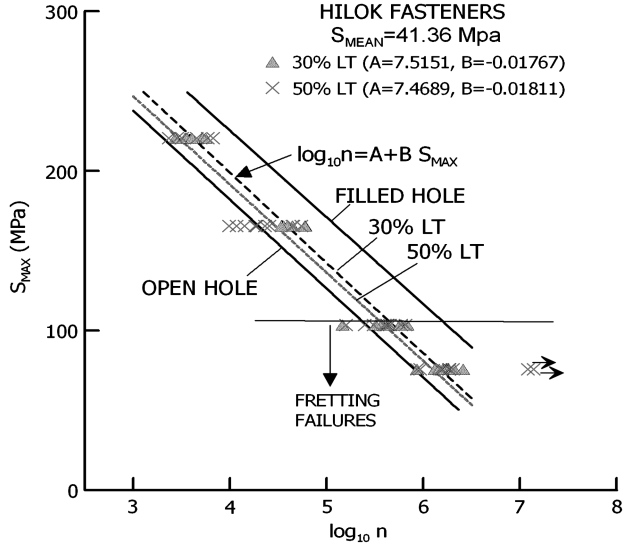

Fig. 14 Fatigue data and best-fit curves for load transfer specimens (Hi-Lok) at $S_{mean} = 41.36$ MPa.

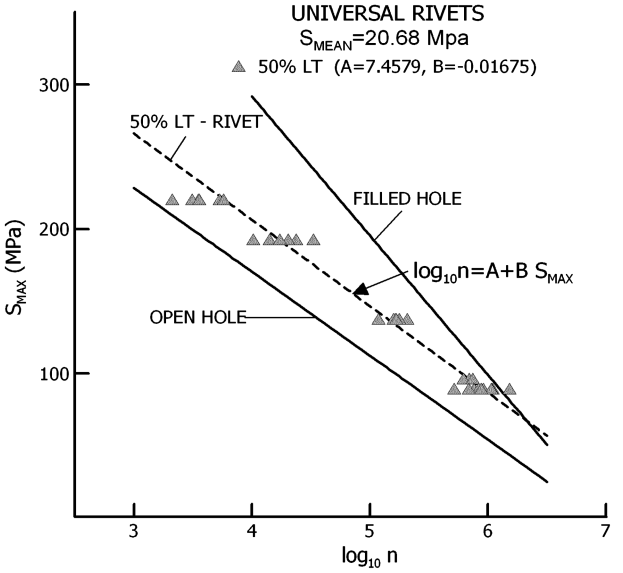

Fig. 15 Fatigue data and best-fit curves for load transfer specimens (rivet) at $S_{mean} = 20.68$ MPa.

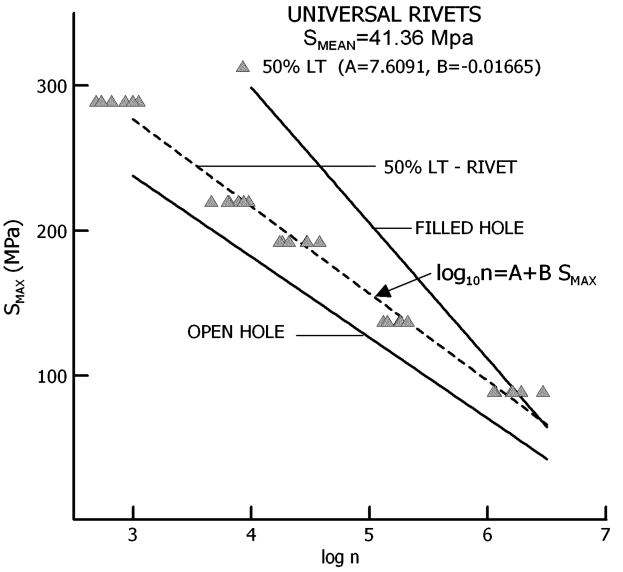

Fig. 16 Fatigue data and best-fit curves for load transfer specimens (rivet) at $S_{mean} = 41.36$ MPa.

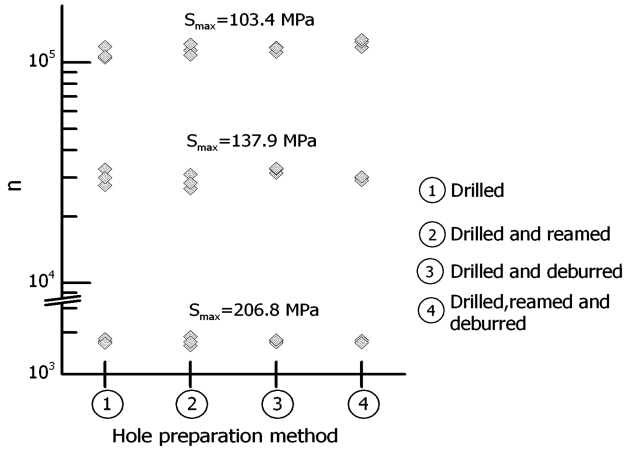

Fig. 17 Comparison of fatigue lives for open-hole specimens with different hole-preparation methods.

their respective curve fits in Figs. 11 and 12, respectively. Based on these two figures, it may be observed that the fatigue life increases with increase in mean stress level, which is consistent with the trends reported by Illg [23] for notched 2024-T3 and 7075-T6 aluminum alloys. The beneficial effects of hole filling is also evident from these figures. The increase in fatigue life can be attributed to the reduction is stress range and the increase in mean stress level that occurs locally due to hole filling [10,24]. During the compression phase of the loading, the fastener shank is compressed between the hole, thus providing an alternate load path that alleviates the stress concentration at the hole boundary. Because of the reduction in the magnitude of the compressive stress, the stress range decreases and the mean stress level increases locally. The scenario is now equivalent to an open-hole specimen subjected to a higher mean stress level, which implies an increase in fatigue life.

The differences between the fatigue lives of filled-hole specimens using Hi-Lok fasteners and rivets may be attributed to the interference levels and Young's modulii of the fastener material. With similar interference levels, a higher filled-hole fatigue life would be expected for the Hi-Lok fastener, due to its higher Young's modulus when compared to that of the rivet, since the load transmitted through the hole by compression of fastener shank would be proportional to the fastener modulus. However, the interference levels were different for the Hi-Lok and rivet filled-hole specimens used in this study. The aluminum rivets expanded during the installation process and filled the hole. On the other hand, in addition to the clearance hole used in this study, the clamping force generated during installation of the Hi-Lok somewhat reduces the hole-filling effect of the fastener (due to Poisson contraction of the fastener shank) unless an interference hole is used. At lower fatigue stress levels, the differences between the Hi-Lok and rivet filled-holes were observed to be insignificant, as the relative effects of fastener modulus and interference levels tend to produce similar hole-filling effects. However, at the higher fatigue stress levels, the effects of using a clearance hole seem to override the beneficial effects of the fastener stiffness, resulting in lower fatigue lives for Hi-Lok filled-hole specimens.

From a load transfer point of view, the filled-hole configuration represents the zero-load-transfer case. Strictly speaking, the specimens should include the load transfer part to capture the clamp-up friction-induced fretting failures that could occur in load transfer specimens [7,14]. The load transfer part in this case will be a simple pad that ensures zero load transfer [14]. However, this was neglected to simplify the specimen configuration and should be addressed in the future.

The fatigue lives of load transfer specimens at the two mean stress levels investigated and the corresponding best-fit curves are plotted in Figs. 13 and 14 for the Hi-Lok fasteners and in Figs. 15 and 16 for the riveted specimens. The S_{MAX}-vs-log-life curves for the corresponding open-hole and filled-hole specimens are superposed on the figures for comparison. Based on the figures, the mean lives of the load transfer specimens approach that of the open-hole configuration, with increasing load transfer level. The observed trends are similar to those of [8], in which the fatigue life decreases with load transfer level, with the exception that the lives are still comparable to the open-hole case or better. A possible reason could be the choice of mean stress levels used in this study, unlike Lee's [8] work, in which a stress ratio of $R = 0.05$ was maintained in all tests.

C. Failure Modes

The failure modes of load transfer specimens were dependent on the fastener type, load transfer levels, S_{mean}, and S_{max}. The test specimens were carefully disassembled after failure and the fractured surfaces and the faying surfaces around the hole were examined. The net-section failure was dominant at the higher S_{max} irrespective of the fastener type, load transfer, and stress levels. Examination of the fractured surface did not reveal information about fatigue crack initiation sites, due to the smudging of the fracture surface by the compressive loads. Pictures of the faying surfaces around the fastener hole of the main parts of MLT specimens are shown in Fig. 18. The specimens using Hi-Lok fasteners exhibited a very rough friction zone (gouging) around the hole when compared to the riveted specimen. This is due to the higher clamping forces associated with a Hi-Lok fastener, the clad layer, and the use of clearance holes, which facilitates more relative motion between the main and load transfer parts. The net-section fracture mode passing through the hole was characteristic of specimens failing below 10^5 cycles. At the lower S_{max} levels, the failure mode in Hi-Lok specimens changed to a fretting-induced failure mode, with the fracture occurring at a characteristic distance (edge of the fastener head) away from the hole on the load introduction side of the specimen [7,19].

The fretting failures occurring on the load introduction sides of the specimen are consistent with the observations reported in [10], in which larger rubbing movements produced higher reductions in fatigue strength. The figure shows the region around the hole on the faying surface of the main part. The surface around the hole was smoother than that at the higher S_{max}, but distinct spots of oxide debris were observed away from the fastener hole. The fretting failures occurring away from the hole exhibited dependence on both mean stress and load transfer level. At the mean stress level of 20.68 and $S_{max} = 103$ MPa, the ILT specimens failed due to fretting at the edge of the clamp-up region, whereas the MLT specimens failed by crack propagation across the minimum section. However, at the mean stress of 41.36 MPa, both ILT and MLT specimens failed due to fretting initiated failure at the edge of the clamp-up region.

Unlike the specimens with a Hi-Lok fastener, the riveted fasteners failed in a net-section fracture mode at all maximum stress levels used in this study. The oxide debris was present even in riveted specimens at the lower S_{max} (see Fig. 18b), but the distribution of this debris was different from that in the Hi-Lok specimens. The oxide debris was localized to regions at the edge and outside of the clamping region in specimens using Hi-Lok fasteners, whereas it encompassed the hole in riveted specimens. The failure modes observed for the two fastener types in this study are consistent with the observations of Palmberg et al. [19].

D. Generation of Empirical Factors β and θ

The best-fit fatigue-life curves generated using the experimental data were used to compute the empirical factors β and θ for the different combinations of fasteners and load transfer levels. The

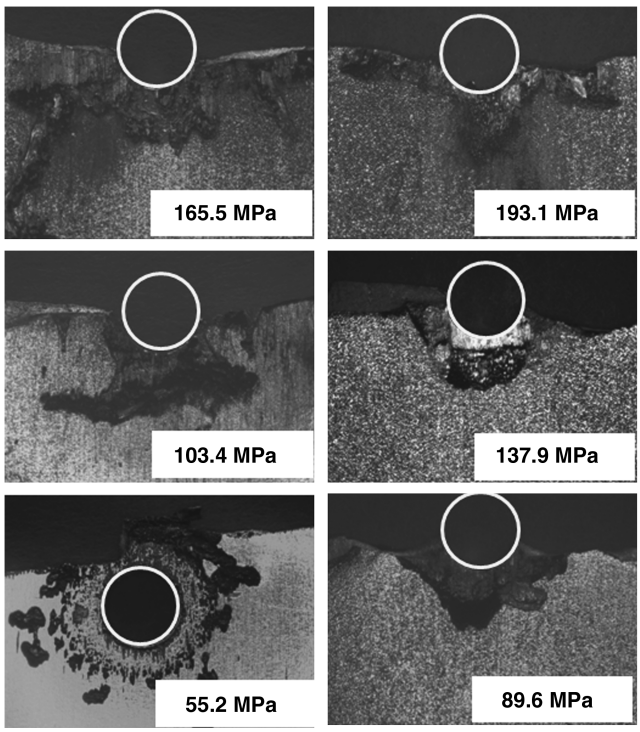

a) Hilok b) Rivet

Fig. 18 Observed failure modes in MLT specimens at a mean stress of 20.68 MPa and different maximum stress levels.

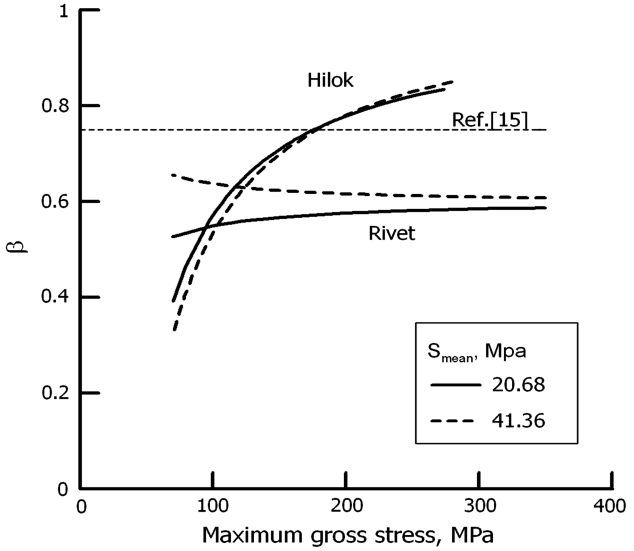

Fig. 19 Hole-filling factor β for Hi-Lok fasteners and rivets.

factors were obtained by successive application of Eq. (3) to the filled-hole and load transfer data, as described previously.

The variation of the hole-filling factor for the Hi-Lok fasteners and rivets as a function of the maximum gross stress is plotted in Fig. 19. The β value for rivets tended to be independent of the maximum gross stress but exhibited a slight dependence on mean stress. On the other hand, the hole-filling factor for Hi-Lok fasteners was dependent on maximum stress level but relatively insensitive to the mean stress. This could be due to the oversized hole used for Hi-Lok fasteners and the higher material stiffness associated with these fasteners. In any case, the hole-filling factors for Hi-Lok fasteners and rivets differ from the reported constant value of 0.75 [15]. The hole-filling factor presented herein is a quantitative measure of the influence of variables such as fastener material and interference/clearance level on the fatigue strength of the filled hole. A detailed investigation with different fastener materials and interference levels would be necessary to further resolve the effects of the variables involved.

The variation of bearing factor θ as a function of applied maximum gross stress is plotted in Fig. 20. For the t/d ratio used in this study, θ should approach a value of 1.5 if the fatigue damage is indeed due to the superposition of bearing and bypass stresses [14]. A bearing factor that is different from its elastic counterpart indicates the presence of other mechanisms of fatigue damage. In the current study, clamp-up-induced friction and hole filling play an important role. For the MLT specimen with rivets, the bearing factor increases with $S_{\max}$ at both the mean stress levels. At the lower $S_{\max}$, the clamp-up friction dominates the behavior in spite of the good hole filling, resulting in a low θ value. Although it is well known that the clamp-up forces in riveted joints are almost nonexistent, the presence of the soft cladding layer and the observed friction region on the faying surfaces around fastener holes (see Fig. 18) indicate that friction cannot be neglected, at least at the lower stress levels. However, with increasing $S_{\max}$, the bearing factor approaches unity as the friction at the faying surfaces is overcome and bearing dominates.

Unlike the riveted specimens, the bearing factor for load transfer specimens using Hi-Lok fasteners was observed to decrease with increasing $S_{\max}$ levels. The θ values for specimens using Hi-Lok fasteners were also lower in comparison to the riveted specimens. This is due to the higher clamp-up forces and the use of clearance holes, both of which promote frictional load transfer. Based on Fig. 20, the contribution of friction to the load transfer process increases with load transfer level, as indicated by the lower θ values for the MLT specimens. The effects of friction in the load transfer process must be further studied/verified using experiments with instrumented fasteners [1] and finite element analysis to better understand the observed trends.

Using the hole-filling and bearing factors for the load transfer specimens, the SSF can be computed as a function of $S_{\max}$. The SSFs for the load transfer specimens are plotted at the mean stress levels of 20.68 and 41.36 MPa in Figs. 21 and 22, respectively. The SSF represents the fatigue factor relative to the open-hole configuration, which has been assigned a value equal to its stress concentration factor K_{tg}. The plots also show the SSF value for the filled-hole configurations, which represent the case of zero load transfer. The SSF values for the filled-hole case reduce to the product of the hole-filling factor and the stress concentration factor [14,15], and thus the trends are similar to that of β. The SSF for the load transfer coupons increase with $S_{\max}$ and approach the open-hole value. At $S_{\text{mean}} = 20.68$ MPa, for the Hi-Lok fastener joints, the SSF is lower for MLT in comparison to ILT at higher $S_{\max}$, whereas the opposite is true at lower stress levels . However, at $S_{\text{mean}} = 41.36$ MPa, for the Hi-Lok fastener joints, the trends are well established with the SSF for the MLT specimens, being consistently higher than the ILT specimens for the range of $S_{\max}$ investigated. A majority of the test data presented in this paper corresponds to $R < 0$. One should exercise caution when extending the observed trends to positive stress ratios, where bearing could dominate [8]. Additional experiments at other mean stress levels are necessary to ensure that the differences observed at the two mean stress levels are not associated

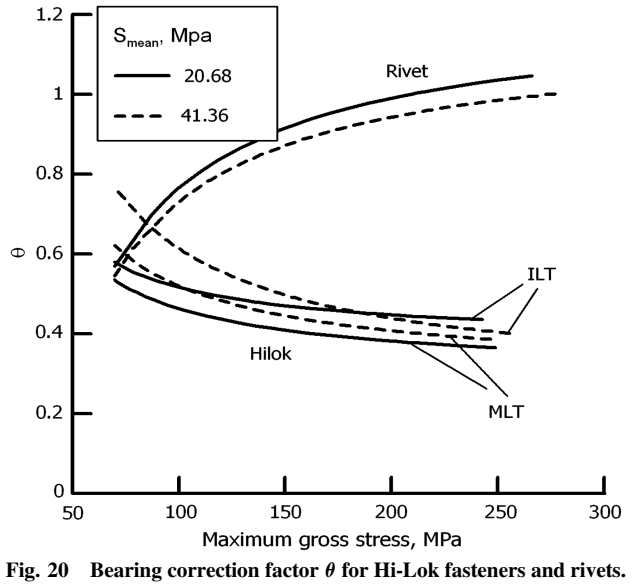

Fig. 20 Bearing correction factor θ for Hi-Lok fasteners and rivets.

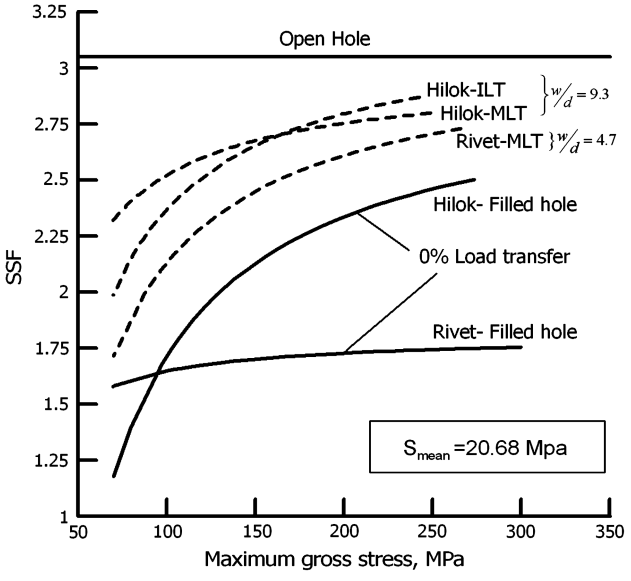

Fig. 21 Stress severity factor for load transfer specimens at $S_{\text{mean}} = 20.68$ MPa.

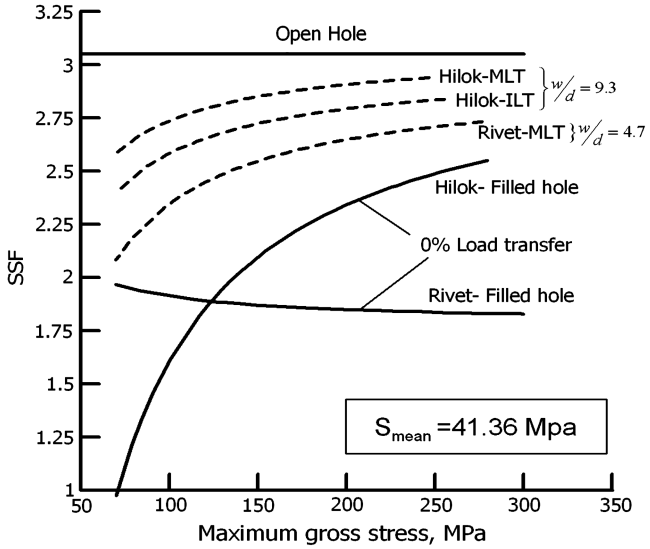

Fig. 22 Stress severity factor for load transfer specimens at S_{mean} = 41.36 MPa.

with experimental scatter, but rather represent the true behavior of the load transfer specimens. The SSF for the riveted MLT specimens was consistently lower than the specimens with a Hi-Lok fasteners, as shown in Figs. 21 and 22. The specimens using rivets were narrower, and thus the magnitude of load transferred through the rivets is lower than with the Hi-Lok fasteners for the same far-field stress level, which explains the lower SSF values.

The *S–n* curves, empirical factors, and SSF presented in this paper correspond to the mean life associated with the particular specimen configuration. The observed trends for the empirical factors and SSF are tied to the specific choice of the *S–n* equation. In addition, the inclusion of run-outs in the curve fitting process may change the observed trends, especially at the higher and lower limits of S_{max} used in the study. Although the use of SSF along with a damage-summation rule might sound attractive for life-prediction purposes, the change in failure modes and the roughness of the faying surfaces at different stress levels should be of particular concern. Based on the experimental observations, overload cycles would increase the surface roughness and thus the friction coefficient at the faying surfaces. The resulting load transferred by the fastener and fatigue life at lower stress levels could be different from that observed in this investigation. A study on the influence of overload cycles may be warranted to augment the use of data presented in this paper.

V. Conclusions

The constant-amplitude fatigue behavior of open-hole, filled-hole, and load transfer specimens fabricated using clad 2024-T3 aluminum was characterized experimentally at two mean stress levels. The fatigue life of load transfer specimens exceeded the life of open-hole configuration in most cases. The load transfer coupons failed in two characteristic failure modes, with net-section fracture dominating at higher stress levels and fretting-induced fracture occurring at lower stress levels. The current study shows that in spite of the clearance holes, the fatigue life of fastener joints with high clamp-up force will be higher than the open-hole scenario. The fatigue-life data have been used to develop fatigue-life-based empirical factors β and θ, which were hitherto based on elastic analysis. These empirical factors were further used to compute the SSF or fatigue quality for the load transfer specimens. The hole-filling factor β was observed to be relatively unaffected by maximum stress level for riveted specimens but exhibited an increasing trend for specimens with a Hi-Lok fasteners. The SSF exhibited dependence on both load transfer and mean stress levels. Additional experiments at a lower load transfer level and positive stress ratios must be conducted to establish the utility of the SSF in life prediction.

Acknowledgments

The work presented in this paper was funded by the Federal Aviation Administration William J. Hughes Technical Center through a research grant. The authors would like to acknowledge the useful inputs of M. Reyer and F. Abali of the Federal Aviation Administration. The authors thank J. S. Tomblin, Executive Director, National Institute for Aviation Research (NIAR), for providing the lab facilities and Lamia Salah, Manager, Fatigue and Fracture Laboratories of NIAR, for efficient coordination/scheduling of the test equipment. The authors appreciate the efforts of Kim-Leng Poon, K. Bangalore, and Damitha Abeywerdana in machining and testing the coupons.

References

[1] Ricci Moretti, L. U., Segerfröjd, G., and Palmberg, B., "Fatigue Behavior of Mechanical Joints—A Programme Overview and an Introduction to Fretting and Fretting Fatigue with Special Application to Joints," Aeronautical Research Inst. of Sweden, TN 1998-03, Bromma, Sweden, 1998.

[2] Segerfröjd, G., Wang, G. S., Palmberg, B., and Blom, A. F., "Fatigue Behavior of Mechanical Joints: Critical Experiments and Statistical Analyses," *ICAF 97: Fatigue in New and Ageing Aircraft: Proceedings of the 19th Symposium of the International Committee on Aeronautical Fatigue*, Engineering Materials Advisory Services, Clifton-upon-Teme, England, U.K., 18–20 June 1997, pp. 575–598.

[3] deCastro, P. M. S. T., deMatos, P. F. P., Moreira, P. M. G. P., and daSilva, L. F. M., "An Overview of the Fatigue Analysis of Aeronautical Structural Details: Open Hole, Single Rivet Lap-Joint, and Lap-Joint Panel," *Materials Science and Engineering A*, Vols. 468–470, Nov. 2007, pp. 144–157. doi:10.1016/j.msea.2006.06.147

[4] Liu, J., Shao, X. J., Liu, Y. J., Liu, Y. S., and Yue, Z. F., "The Effect of Holes Quality on Fatigue Life of Open Hole," *Materials Science and Engineering A*, Vol. 467, Nos. 1–2, 2007, pp. 8–14. doi:10.1016/j.msea.2007.02.060

[5] Liu, J., Yue, Z. F., and Liu, Y. S., "Surface Finish of Open Holes on Fatigue Life," *Theoretical and Applied Fracture Mechanics*, 47, No. 1, 2007, pp. 35–45. doi:10.1016/j.tafmec.2006.10.008

[6] Lanciotti, A., and Polese, C., "The Effect of Interference-Fit Fasteners on the Fatigue Life of Central Hole Specimens," *Fatigue and Fracture of Engineering Materials and Structures*, Vol. 28, No. 7, 2005, pp. 587–597. doi:10.1111/j.1460-2695.2005.00902.x

[7] "Fatigue Rated Fastener Systems," AGARD, Rept. 721, Neuilly-sur-Seine, France, 1985.

[8] Lee, E. U., "Effect of Load Transfer on Fatigue of Mechanically Fastened Metallic Joints," *Fatigue in Mechanically Fastened Composite and Metallic Joints*, edited by J. M. Potter, American Society for Testing and Materials, ASTM STP 927, Philadelphia, 1986, pp. 95–117.

[9] Starikov, R., "Fatigue Behavior of Mechanically Fastened Aluminum Joints Tested in Spectrum Loading," *International Journal of Fatigue*, Vol. 26, No. 10, 2004, pp. 1115–1127. doi:10.1016/j.ijfatigue.2004.03.006

[10] Schijve, J., *Fatigue of Structures and Materials*, Kluwer Academic, Norwell, MA, 2001.

[11] Wang, G. S., "Computational Method for Evaluating The Fatigue Life of Mechanical Joints," *Design for Durability in the Digital Age. Proceedings of the 21st Symposium of International Committee on Aeronautical Fatigue*, edited by J. Rouchon, Engineering Materials Advisory Services, Clifton-upon-Teme, England, U.K., June 2001, pp. 597–625.

[12] Barrios, W., "Stresses and Displacements due to Load Transfer by Fasteners in Structural Assemblies," *Engineering Fracture Mechanics*, Vol. 10, No. 1, 1978, pp. 115–176. doi:10.1016/0013-7944(78)90055-3

[13] Homan, J., and Jongebreur, A. A., "Calculation Method for Predicting the Fatigue Life of Riveted Joints," *Durability and Structural Integrity of Airframes. Proceedings of the 17th ICAF Symposium*, edited by Blom, A. F., Engineering Materials Advisory Services, Clifton-upon-Teme, England, U.K., 1993, pp. 175–190.

[14] Jarfall, L. E., *Optimum Design of Joints: The Stress Severity Factor Concept*, Aeronautical Research Inst. of Sweden, Bromma, Sweden, 1967.

[15] Niu, M. C. Y., *Airframe Structural Design*, Conmilit Press, Hong Kong, 1993.

[16] *Metallic Material Properties Development and Standardization (MMPDS-01)*, U.S. Dept. of Transportation, 2003.
[17] Multipurpose TestWare, Software Package, Ver. 3.5C1817, MTS Systems Corp., Eden Prairie, MN, 2005.
[18] Park, C. Y., and Grandt, A. F., Jr., "A Proposed Fatigue Test Protocol for Generic Mechanical Joints," *Engineering Failure Analysis*, Vol. 13, No. 1, 2006, pp. 136–154. doi:10.1016/j.engfailanal.2004.10.013
[19] Palmberg, B., Segerfröjd, G., Wang, G. S., and Blom, A. F., "Fatigue Behavior of Mechanical Joints: Critical Experiments and Numerical Modelling," *ICAF 95: Estimation, Enhancement and Control of Aircraft Fatigue Performance. Proceedings of the 18th Symposium of the International Committee on Aeronautical Fatigue*, Engineering Materials Advisory Services, Clifton-upon-Teme, England, U.K., 3–5 May 1995, pp. 155–178.
[20] TableCurve 2D, Software Package, Ver. 5.0.1, Systat Software, Inc., Richmond, CA, 2002.
[21] Nelson, W., "Fitting of Fatigue Curves with Nonconstant Standard Deviation to Data with Runouts," *Journal of Testing and Evaluation*, Vol. 12, No. 2, March 1984, pp. 69–77. doi:10.1520/JTE10700J
[22] Pascaul, F. G., and Meeker, W. Q., "Analysis of Fatigue Data with Runouts Based on a Model with Nonconstant Standard Deviation and a Fatigue Limit Parameter," *Journal of Testing and Evaluation*, Vol. 25, No. 3, March 1997, pp. 292–301. doi:10.1520/JTE11341J
[23] Illg, W., "Fatigue Tests on Notched and Unnotched Sheet Specimens of 2024-T3 and 7075-T6 Aluminum Alloys and of SAE 4130 Steel with Special Consideration of the Life Range from 2 to 10,000 Cycles," NACA, TN 3866, 1956.
[24] Manson, S. S., and Halford, G. R., *Fatigue and Durability of Structural Materials*, ASM International, Materials Park, OH, 2006.